N-Donor Effects on Carboxylate Binding in Mononuclear Iron(II) Complexes of a Sterically Hindered Benzoate Ligand

John R. Hagadorn, Lawrence Que, Jr.,* and William B. Tolman*

207 Pleasant St S.E., Department of Chemistry and Center for Metals in Biocatalysis, University of Minnesota, Minneapolis, Minnesota 55455

Received May 19, 2000

Using the sterically hindered 2,6-dimesitylbenzoate ligand $Mes_2ArCO_2^-$, a series of mononuclear Fe(II) carboxylate complexes has been obtained with the general formula $(Mes_2ArCO_2)_2Fe(base)_2$ (base = 1-methylimidazole (MeIm), pyridine (Py), 2-picoline (2-Pic), 2,5-lutidine (2,5-Lut), 2,6-lutidine (2,6-Lut), $(base)_2$ = *N*,*N*,*N*′,*N*′-tetramethylethylenediamine (TMEDA)). For the monodentate base adducts, single-crystal X-ray diffraction studies revealed several different structural types ranging from distorted tetrahedral to distorted octahedral that correlate with the degree of α-substitution of the N-donors. Increasing α-substitution leads to the lengthening of the Fe−N bond, which in turn results in a change in carboxylate binding mode from η^1 to η^2. We surmise that this change is due to an electrostatic effect and is driven by increasing the Lewis acidity of the Fe center. Such a simple process for inducing carboxylate shifts could play a critical role in biological systems.

Introduction

Carboxylate ligation plays a variety of critical roles in mono- and dinuclear Fe-containing metalloproteins.[1] In addition to providing anionic donors to the metal center, carboxylate residues may adopt a variety of binding modes, thus providing a flexible binding environment that yields multiple coordination motifs. This phenomenon is well documented for the O_2-activating non-heme diiron enzymes such as methane monooxygenase (MMO), ribonucleotide reductase (RNR), and stearoyl-ACP Δ^9-desaturase (Δ9D). For MMO and RNR, crystallographic[2] and EXAFS[3] studies have revealed dramatic changes in carboxylate binding geometries[4] and Fe−Fe distances ($\Delta \approx 1.7$ Å) for species that are involved in their catalytic cycles. Similarly, the addition of substrate to Δ9D has been shown to induce changes in coordination number and stereochemistry that likely include a change in carboxylate binding mode from bidentate to monodentate.[5] While core flexibility is undoubtedly essential for the formation of reactive intermediates for these diiron enzymes, it is less clear whether similar processes play integral roles in the chemistry of mononuclear Fe active sites supported by carboxylates. It is noteworthy that both mono- and bidentate carboxylates have been identified in X-ray structures of mononuclear Fe centers in proteins.[6]

To better understand the roles that supporting ligands play in the aforementioned systems and ultimately improve our understanding of metalloenzyme mechanism, we[7] and others[8] have been interested in studying Fe carboxylate complexes that

(1) For recent review articles, see: (a) Lange, S. J.; Que, L., Jr. *Curr. Opin. Chem. Biol.* **1998**, *2*, 159−172. (b) Que, L., Jr.; Ho, R. Y. N. *Chem. Rev.* **1996**, *96*, 2607−2624. (c) Wallar, B. J.; Lipscomb, J. D. *Chem. Rev.* **1996**, *96*, 2625−2658. (d) Feig, A. L.; Lippard, S. J. *Chem. Rev.* **1994**, *94*, 759−805.

(2) (a) Eklund, H.; Eriksson, M.; Uhlin, U.; Nordlund, P.; Logan, D. *J. Biol. Chem.* **1997**, *378* (8), 821−825 and references contained within. (b) Andersson, M. E.; Högbom, M.; Rinaldo-Matthis, A.; Andersson, K. K.; Sjöberg, B.-M.; Nordlund, P. *J. Am. Chem. Soc.* **1999**, *121*, 2346−2352. MMO structures: (c) Rosenzweig, A. C.; Nordlund, P.; Takahara, P. M.; Frederick, C. A.; Lippard, S. J. *Chem. Biol.* **1995**, *2*, 409−418. (d) Rosenzweig, A. C.; Frederick, C. A.; Lippard, S. J.; Nordlund, P. *Nature* **1993**, *366*, 537−543. (e) Elango, N.; Radhakrishnan, R.; Froland, W. A.; Wallar, B. J.; Earhart, C. A.; Lipscomb, J. D.; Ohlendorf, D. H. *Protein Sci.* **1997**, *6*, 556−568.

(3) (a) Riggs-Gelasco, P. J.; Shu, L.; Chen, S.; Burdi, D.; Huynk, B. H.; Que, L., Jr.; Stubbe, J. *J. Am. Chem. Soc.* **1998**, *120*, 849−860. (b) Shu, L.; Nesheim, J. C.; Kauffmann, K.; Münck, E.; Lipscomb, J. D.; Que, L., Jr. *Science* **1997**, *275*, 515−518.

(4) Rardin, R. L.; Tolman, W. B.; Lippard, S. J. *New J. Chem.* **1991**, *15*, 417−430.

(5) (a) Yang, Y.-S.; Broadwater, J. A.; Pulver, S. C.; Fox, B. G.; Solomon, E. I. *J. Am. Chem. Soc.* **1999**, *121*, 2770−2783. (b) Broadwater, J. A.; Achim, C.; Münck, E.; Fox, B. G. *Biochemistry* **1999**, *38*, 12197−12204.

(6) (a) Kauppi, B.; Lee, K.; Carredano, E.; Parales, R. E.; Gibson, D. T.; Eklund, H.; Ramaswamy, S. *Structure* **1998**, *6*, 571−586. (b) Han, S.; Eltis, L. D.; Timmis, K. N.; Muchmore, S. W.; Bolin, J. T. *Science* **1995**, *270*, 976−980. (c) Senda, T.; Sugiyama, K.; Narita, H.; Yamamoto, T.; Kimbara, K.; Fukuda, M.; Sato, M.; Yano, K.; Mitsui, Y. *J. Mol. Biol.* **1996**, *255*, 735−752. (d) Boyington, J. C.; Gaffney, B. J.; Amzel, M. *Science* **1993**, *260*, 1482−1486. (e) Minor, W.; Steczko, J.; Bolin, J. T.; Otwinowski, Z.; Axelrod, B. *Biochemistry* **1993**, *32*, 6320−6323. (f) Roach, P. L.; Clifton, I. J.; Fülöp, V.; Harlos, K.; Barton, G. J.; Hajdu, J.; Andersson, I.; Schofield, C. J.; Baldwin, J. E. *Nature* **1995**, *375*, 700−704.

(7) (a) Hagadorn, J. R.; Que, L., Jr.; Tolman, W. B. *J. Am. Chem. Soc.* **1998**, *120*, 13531−13532. (b) Hagadorn, J. R.; Que, L., Jr.; Tolman, W. B. *J. Am. Chem. Soc.* **1999**, *121*, 9760−9761.

(8) Selected examples of carboxylate-rich Fe complexes: (a) Du Bois, J.; Mizoguchi, T. J.; Lippard, S. J. *Coord. Chem. Rev.* **2000**, *200−202*, 443−485 and references contained within. (b) Hagen, K. S.; Lachicotte, R. *J. Am. Chem. Soc.* **1992**, *114*, 8741−8742. (c) Randall, C. R.; Shu, L.; Chiou, Y. M.; Hagen, K. S.; Ito, M.; Kitajima, N.; Lachicotte, R. J.; Zang, Y.; Que, L., Jr. *Inorg. Chem.* **1995**, *34*, 1036−1039. (d) Mizoguchi, T. J.; Davydov, R. M.; Lippard, S. J. *Inorg. Chem.* **1999**, *38*, 4098−4103. (e) LeCloux, D. D.; Barrios, A. M.; Mizoguchi, T. J.; Lippard, S. J. *J. Am. Chem. Soc.* **1998**, *120*, 9001−9014. (f) D. Lee, S. J. Lippard, *J. Am. Chem. Soc.* **1998**, *120*, 12153−12154. (g) Lee, D.; DuBois, J.; Petasis, D.; Hendrich, M. P.; Krebs, C.; Huynh, B. H.; Lippard, S. J. *J. Am. Chem. Soc.* **1999**, *121*, 9893−9894. (h) Beer, R. H.; Tolman, W. B.; Bott, S. G.; Lippard, S. J. *Inorg. Chem.* **1991**, *30*, 2082−2092. (i) Coucouvanis, D.; Reynolds, R. A., III.; Dunham, W. R. *J. Am. Chem. Soc.* **1995**, *117*, 7570−7571. (j) Singh, B.; Long, J. R.; Papaefthymiou, G. C.; Stavropoulos, P. *J. Am. Chem. Soc.* **1996**, *118*, 5824−5825. (k) Singh, B.; Long, J. R.; deBiani, F. F.; Gatteschi, D.; Stavropoulos, P. *J. Am. Chem. Soc.* **1997**, *119*, 7030−7047. (l) Cai, L.; Han, Y.; Mahmoud, H.; Xie, W.; Segal, B. M. *Inorg. Chem. Commun.* **1998**, *1*, 71−76.

(9) So, J.-H., Boudjouk, P. *Inorg. Chem.* **1990**, *29*, 1592−1593.

10.1021/ic000531o CCC: $19.00
Published on Web 11/30/2000

model features of various Fe-containing metalloenzymes. To this end, we are using sterically hindered benzoate ligands to control coordination number and nuclearity in mono- and dinuclear Fe(II) carboxylates. Our previously reported results have focused on diferrous derivatives and novel mixed-valence diiron complexes prepared with the 2,6-dimesitylbenzoate ligand ($Mes_2ArCO_2^-$).[7] Here we present a unique series of structurally characterized *mononuclear* Fe(II) carboxylates prepared with simple mono- and bidentate N-donors. These complexes greatly expand the list of known structure types for Fe(II) carboxylates, and include coordinatively unsaturated species made accessible by the extremely bulky nature of the supporting ligands. We have also identified a correlation between the structure type and the degree of α-substitution in a series of related N-donors, thus providing insights into the manner by which N-donors may affect carboxylate binding modes and geometry at mononuclear Fe centers. A small portion of this work was reported in a communication.[7a]

Experimental Section

General Considerations. All manipulations were carried out under nitrogen using standard Schlenk-line and glovebox techniques. Tetrahydrofuran (THF), toluene, diethyl ether, and pentane were distilled from Na/benzophenone. Hexamethyldisiloxane (HMDSO) and *N,N,N′,N′*-tetramethylethylenediamine (TMEDA) were distilled from Na. Dichloromethane, acetonitrile, and 1-methylimidazole (MeIm) were distilled from CaH_2. Pyridine (Py), 2-picoline (2-Pic), 2,5-lutidine (2,5-Lut), and 2,6-lutidine (2,6-Lut) were vacuum distilled from CaH_2. $CDCl_3$ was vacuum transferred from CaH_2. $Mes_2ArCO_2Li(solvent)_n$ was prepared as described,[7a] but better yields (>95%) of crystalline product were obtained by the addition of CH_3CN to concentrated Et_2O solutions of the lithium carboxylate followed by cooling to −40 °C. For individual batches, solvent content and composition were determined by ^{1}H NMR spectroscopy. Commercial $FeCl_2$ was dried by treatment with Me_3SiCl.[9] $Fe(OTf)_2{\cdot}2CH_3CN$ (OTf = O_3SCF_3) was prepared by the addition of 2.2 equiv of Me_3SiOTf to $FeCl_2$ in 2:1 CH_2Cl_2/CH_3CN, followed by crystallization from CH_3CN/Et_2O. $[(TMEDA)FeCl_2]_2$[10] was prepared by the addition of 1.1 equiv of TMEDA to a CH_2Cl_2 suspension of anhydrous $FeCl_2$ followed by crystallization at −40 °C. ^{1}H NMR spectra of Fe complexes were acquired on ca. 4 mM $CDCl_3$ solutions using a 500 MHz Varian spectrometer. Selected acquisition parameters for paramagnetic complexes: relaxation delay = 0.03 s, acquisition time = 0.064 s, line broadening = 30 Hz, sweep width = 100−250 ppm. Chemical shifts (δ) are given relative to residual protium in the deuterated solvent at δ 7.24 ppm for $CDCl_3$. Line widths at half peak height ($\omega_{1/2}$) are reported in hertz. Elemental analyses were determined by Atlantic Microlab, Inc. Details of X-ray structure determinations and crystallographic information files are presented as Supporting Information.

$(Mes_2ArCO_2)_2Fe(MeIm)_2$. Dichloromethane (10 mL) was added to $FeCl_2$ (52.0 mg, 0.410 mmol) and $(Mes_2ArCO_2)Li(Et_2O)$ (0.334 g, 0.821 mmol) to form a tan suspension, to which MeIm (62.0 mg, 0.76 mmol) was added. After stirring overnight, the volatile materials were removed under reduced pressure. The white solid was extracted with toluene (15 mL) and filtered through a frit. Concentration of the filtrate to 7 mL, addition of pentane (8 mL), and cooling to −30 °C gave the product as colorless microcrystals (70 mg, 20%). ^{1}H NMR ($CDCl_3$): δ ($\omega_{1/2}$, Hz) 58 (380) (MeIm, α-CH), 36 (50) (MeIm, *β*-C*H*), 29 (350) (MeIm, α-C*H*), 15.1 (50) (MeIm NCH_3), 11.8 (50) (Ar, *m*-H), 5.7 (60) (Mes, *m*-H), 2.8 (80) (Mes, *o*-CH_3), 1.4 (60) (Ar, *p*-H), 1.2 (50) (Mes, *p*-CH_3). Anal. Calcd (Found) for $C_{58}H_{62}N_4O_4Fe$: C, 74.51 (74.61); H, 6.68 (6.91); N, 5.99 (5.79).

$(Mes_2ArCO_2)_2Fe(Py)_2{\cdot}CH_2Cl_2$. A mixture of toluene (20 mL) and Py (0.162 g, 2.05 mmol) was added to $Fe(OTf)_2{\cdot}2CH_3CN$ (0.299 g, 0.686 mmol) and $(Mes_2ArCO_2)Li(Et_2O)_{0.25}(CH_3CN)_{0.30}$ (0.542 g, 1.37 mmol) to form a yellow suspension. After stirring overnight, the volatile components were removed under reduced pressure. The resulting yellow solid was extracted with CH_2Cl_2 (25 mL). The cloudy solution was filtered, the filtrate was concentrated to 10 mL, and HMDSO (20 mL) was layered on the solution. After 12 h, yellow crystals had formed. Cooling to −30 °C afforded additional product (0.39 g, 57% yield). ^{1}H NMR ($CDCl_3$): δ ($\omega_{1/2}$, Hz) 142 (870) (Py, α-C*H*), 36 (320) (Py, *β*-C*H*), 12.8 (90) (Ar, *m*-H), 8.5 (80) (Pyr, *γ*-C*H*), 5.2 (70) (Mes, *m*-H), 3.0 (80) (Mes, *o*-CH_3), 1.6 (70) (Ar, *p*-H), 0.7 (60) (Mes, *p*-CH_3). Anal. Calcd (Found) for $C_{60}H_{60}N_2O_4Fe$: C, 72.14 (72.26); H, 6.17 (6.16); N, 2.70 (2.76).

$(Mes_2ArCO_2)_2Fe(2\text{-}Pic)_2$. This complex was prepared analogously to $(Mes_2ArCO_2)_2Fe(Py)_2$. The product was isolated as yellow crystals (40% yield). ^{1}H NMR ($CDCl_3$): δ ($\omega_{1/2}$, Hz) 120.0 (1300) (Pic, α-C*H*), 49.5 (240) (Pic, *β*-C*H*), 33.0 (260) (Pic, *β*-C*H*), 14.8 (190) (Ar, *m*-H), 5.3 (190) (Mes, *o*-CH_3 and *m*-H), 2.6 (150) (Pic, *γ*-H), 0.3 (100) (Mes, *p*-CH_3), −1.6 (240) (Ar, *p*-H), −19.6 (690) (Pic, α-CH_3). Anal. Calcd (Found) for $C_{64}H_{64}N_2O_4Fe$: C, 77.81 (76.82); H, 6.74 (6.74); N, 2.93 (2.96).

$(Mes_2ArCO_2)_2Fe(2,5\text{-}Lut)_2$. This complex was prepared analogously to $(Mes_2ArCO_2)_2Fe(Py)_2$. The product was isolated as yellow crystals (61% yield). ^{1}H NMR ($CDCl_3$): δ ($\omega_{1/2}$, Hz) 125.6 (1600) (Lut, α-C*H*), 47.9 (260) (Lut, *β*-C*H*), 15.7 (260), 6.3 (270), 5.0 (190), 3.2 (200), 1.8 (250) (Lut, *β*-CH_3), −0.2 (160), −2.0 (250), −36.8 (930) (Lut, α-CH_3). Anal. Calcd (Found) for $C_{64}H_{68}N_2O_4Fe$: C, 78.03 (77.48); H, 6.96 (6.95); N, 2.84 (2.91).

$(Mes_2ArCO_2)_2Fe(2,6\text{-}Lut)_2$. This complex was prepared analogously to $(Mes_2ArCO_2)_2Fe(Py)_2$. The product was isolated as colorless crystals (25% yield). ^{1}H NMR ($CDCl_3$): δ ($\omega_{1/2}$, Hz) 40.7 (2000), 32.4 (860), 29.1 (1000), 24.7 (2200), 16.2 (960), 12.0 (1200), 7.1 (400), 2.2 (600), 1.2 (140), −5.8 (510), −25.0 (680), −74.5 (1440). Anal. Calcd (Found) for $C_{64}H_{68}N_2O_4Fe$: C, 78.03 (78.19); H, 6.96 (6.98); N, 2.84 (2.85).

$(Mes_2ArCO_2)_2Fe(TMEDA)$. Dichloromethane (5 mL) and toluene (3 mL) were added to $(Mes_2ArCO_2)Li(Et_2O)$ (0.519 g, 1.29 mmol) to form a cloudy solution. To this solution was added a CH_2Cl_2 solution (5 mL) of $[(TMEDA)FeCl_2]_2$ (0.160 g, 0.319 mmol) to yield a cloudy, pale yellow solution. After stirring overnight, the volatile materials were removed under reduced pressure. The solid was extracted with toluene (15 mL) and filtered through a glass frit. Addition of pentane (10 mL) to the filtrate and cooling to −30 °C gave the product as colorless crystals (total yield from two crops: 0.36 g, 64%). ^{1}H NMR ($CDCl_3$): δ ($\omega_{1/2}$, Hz) 108 (720) (TMEDA, NCH_3), 86 (780) (TMEDA, NCH_2), 13.2 (60) (Ar, *m*-H), 5.4 (100) (Mes, *o*-CH_3), 2.5 (70) (Mes, *m*-H), 1.8 (50) (Ar, *p*-H), −2.2 (60) (Mes, *p*-CH_3). Anal. Calcd (Found) for $C_{56}H_{66}N_2O_4Fe$: C, 75.83 (75.71); H, 7.50 (7.56); N, 3.16 (3.17).

Results

As we reported earlier,[7a] the salt-metathesis reaction of 2 equiv of $(Mes_2ArCO_2)Li(solvent)_n$ with $Fe(OTf)_2{\cdot}2CH_3CN$ (OTf = O_3SCF_3) in toluene/CH_3CN yields the diferrous complex $(Mes_2ArCO_2)_4Fe_2(CH_3CN)_2$ (Scheme 1). When bulkier, more basic N-donors (e.g., MeIm, pyridines, or TMEDA) are added to solutions of the diiron complex, new species form immediately (by ^{1}H NMR, $CDCl_3$) and the diiron complex is no longer observed. These same mononuclear derivatives can be synthesized conveniently in good yields by salt-metathesis reactions in the presence of 2−3 equiv of the bases. The preparation of $(Mes_2ArCO_2)_2Fe(TMEDA)$, which features a bidentate N-donor ligand, was conveniently carried out by reaction of the lithium benzoate with $[(TMEDA)FeCl_2]_2$ in a CH_2Cl_2−toluene mixture. The mesityl groups of the ligands impart the products with good solubility in aromatic hydrocarbon solvents and CH_2Cl_2. All compounds were isolated as either colorless (MeIm, 2,6-Lut, TMEDA) or yellow (Py, 2-Pic, 2,5-Lut) crystalline solids. Combustion analysis revealed that the complexes all share the empirical formula $(Mes_2ArCO_2)_2Fe(base)_2$.

(10) (a) Davies, S. C.; Hughes, D. L.; Leigh, G. J.; Sanders, J. R.; de Souza, J. S. *J. Chem. Soc., Dalton Trans.* **1997**, 1981−1988. (b) Hagadorn, J. R.; Arnold, J.; Unpublished results.

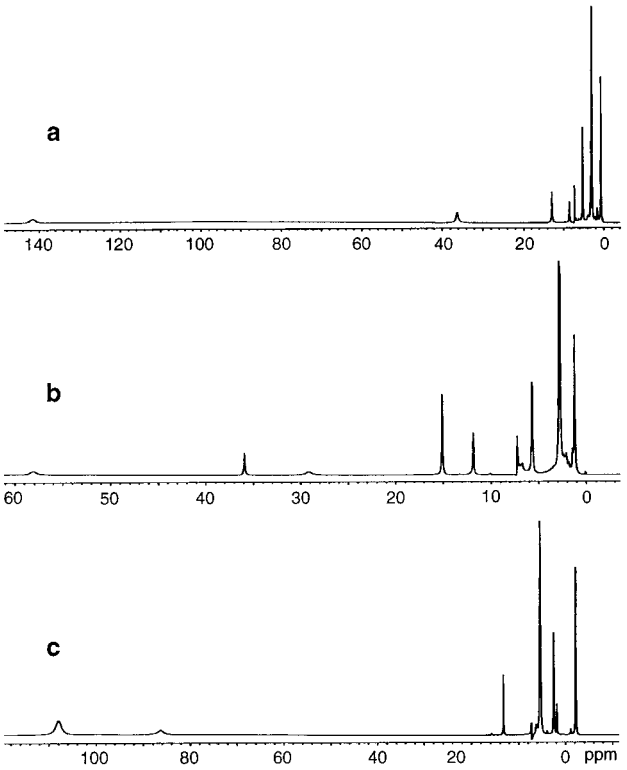

Figure 1. ^{1}H-NMR spectra of $(Mes_2ArCO_2)_2Fe(base)_2$ (a) base = Py, (b) base = MeIm, and (c) $(base)_2$ = TMEDA at 298 K in $CDCl_3$.

Scheme 1

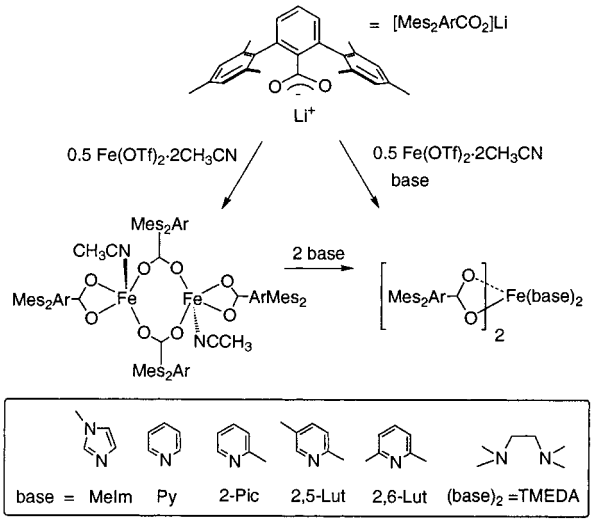

The solid-state structures of all six mononuclear derivatives were determined by single-crystal X-ray diffraction. Although they share the composition of two carboxylates and two N-donors per Fe atom, several distinct structural types were observed. These approximate tetrahedral, trigonal bipyramidal, and octahedral ligand environments. The complexes $(Mes_2ArCO_2)_2Fe(MeIm)_2$[7a] (Figure S7) and $(Mes_2ArCO_2)_2Fe(Py)_2$ (Figure 2) feature similar pseudotetrahedral Fe centers. For the core of the Py adduct, a pair of monodentate carboxylates are bound to Fe with relatively short Fe−O distances of 1.980(2) and 1.961(2) Å for O1 and O3, respectively (Table 1). The other oxygen atoms are much farther removed with Fe−O distances of 2.666(2) and 3.329(2) Å. As expected for the four-coordinate

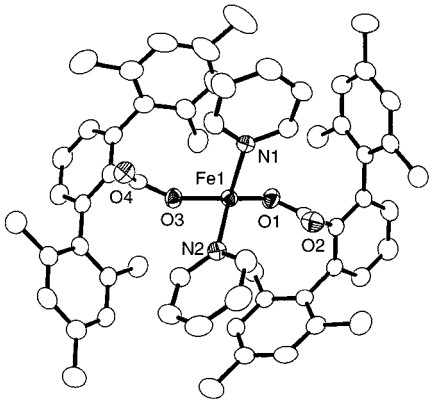

Figure 2. Drawing of the X-ray structure of $(Mes_2ArCO_2)_2Fe(Py)_2$ showing 50% thermal ellipsoids. Hydrogen atoms are omitted for clarity.

complex, the Fe−N bonds are short (2.103(2) and 2.106(2) Å) and the N−Fe−N angle is large at 116.07(9)°.

The compounds $(Mes_2ArCO_2)_2Fe(2,5\text{-Lut})_2$ (Figure 3) and $(Mes_2ArCO_2)_2Fe(2\text{-Pic})_2$ (Figures S2 and S3) are 6-coordinate complexes with *cis*-coordinated N-donors and two bidentate carboxylates. Because these complexes adopt similar structures, only that of the 2,5-Lut derivative will be discussed in detail. The Fe−N bond distances (2.181(2) Å) are longer than those in the unsubstituted Py derivative (average 2.105 Å) due to the α-substitution of the N-donor and a higher overall coordination number. Due to differing trans ligands, the bidentate carboxylates are bound asymmetrically ($\Delta_{FeO} = 0.12$ Å), with the longer Fe−O bonds being trans to the N-donors (Table 1). Their average value of 2.18 Å is considerably longer than those for the aforementioned 4-coordinate complexes (average 1.99 Å).

The addition of a second α-methyl group to the N-donor results in another change of coordination environment. Similar to the aforementioned mono α-substituted Py derivatives, $(Mes_2ArCO_2)_2Fe(2,6\text{-Lut})_2$ forms a 6-coordinate complex, but the N-donors are coordinated trans to each other (Figure 4). The sterically hindered 2,6-Lut has a fairly long Fe−N bond of 2.241(3) Å that is ca. 0.15 Å longer than the Fe−N bonds of $(Mes_2ArCO_2)_2Fe(Py)_2$. Unlike the 2-Pic and 2,5-Lut derivatives, the carboxylates are bound symmetrically with Fe−O distances of 2.189(2) and 2.190(2) Å that are equal within experimental error.

The use of the bidentate N-donor TMEDA yielded yet another coordination geometry in the solid state. As shown in Figure 5, $(Mes_2ArCO_2)_2Fe(TMEDA)$ has a distorted trigonal bipyramidal Fe center ($\tau = 0.26$)[11] with O2 and O3 occupying the pseudoaxial sites (O2−Fe−O3 154.74(8)°). The 5-coordinate complex features one η^2-chelated and one monodentate carboxylate. The bidentate benzoate features Fe−O distances (average 2.149 Å) that are comparable to those found in the aforementioned 6-coordinate derivatives. The monodentate Fe1−O3 bond of 1.924(2) Å, however, is even shorter than those observed for the MeIm and Py adducts. The chelating TMEDA is bound in typical fashion with an N−Fe−N angle of 82.65(8)°, which is smaller than the corresponding values in the other compounds with monodentate N-donors.

^{1}H NMR spectroscopic data in $CDCl_3$ have been obtained for the various complexes to assess the extent to which the solid-state structures are retained in solution. As shown in Figure 1a, b, and c, respectively, $(Mes_2ArCO_2)_2Fe(Py)_2$, $(Mes_2ArCO_2)_2Fe(MeIm)_2$, and $(Mes_2ArCO_2)_2Fe(TMEDA)$ exhibit relatively sharp resonances that span 140 ppm, consistent with the presence of high-spin Fe(II) centers. Tentative assignments for many signals can be made based on integration and by comparison

(11) Addison, A. W.; Rao, T. N.; Reedjik, J.; van Rijn, J.; Verschoor, G. C. *J. Chem. Soc., Dalton Trans.* **1984**, 1349−1356.

Table 1. Line Drawings of Core Structures and Selected Bonds and Angles

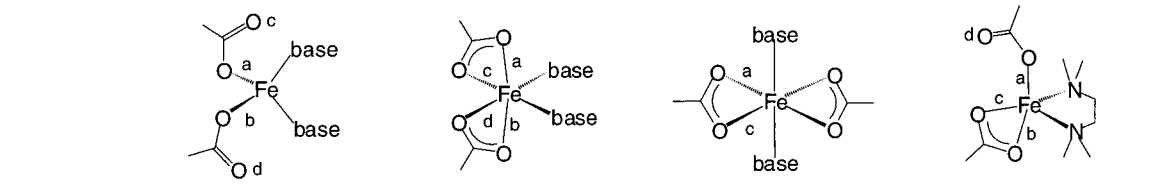

	MeIm	Py	2-Pic (mol. 1)	2-Pic (mol. 2)	2,5-Lut	2,6-Lut	TMEDA
Fe-O distances (Å)							
a	1.989(2)	1.961(2)	2.135(3)	2.088(3)	2.116(2)	2.189(2)	1.924(2)
b	2.028(2)	1.980(2)	2.142(3)	2.154(3)			2.126(2)
c	2.544(2)	2.666(2)	2.219(3)	2.289(3)	2.236(2)	2.190(2)	2.172(2)
d	3.262(2)	3.329(2)	2.204(3)	2.199(3)			3.574(2)
Fe-N distances (Å)	2.057(2)	2.103(2)	2.172(3)	2.184(4)	2.181(2)	2.241(3)	2.189(2)
	2.066(2)	2.106(2)	2.178(4)	2.207(4)			2.193(2)
N-Fe-N (deg)	116.07(9)	103.49(9)	97.6(2)	93.4(2)	90.3(1)	180	82.65(8)

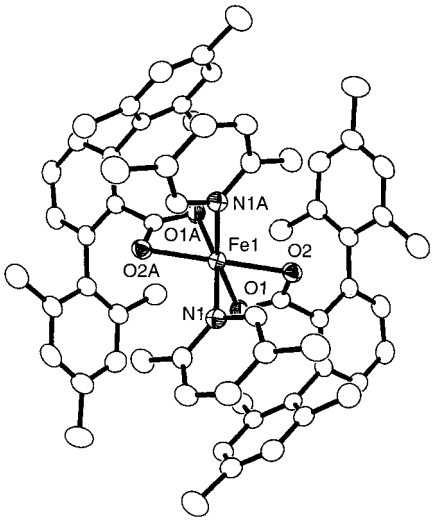

Figure 3. Drawing of the X-ray structure of $(Mes_2ArCO_2)_2Fe(2,5\text{-Lut})_2$ showing 50% thermal ellipsoids. Hydrogen atoms are omitted for clarity.

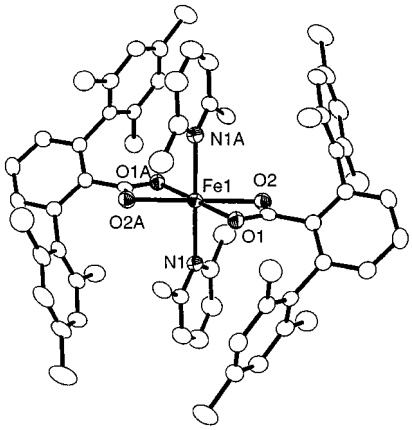

Figure 4. Drawing of the X-ray structure of $(Mes_2ArCO_2)_2Fe(2,5\text{-Lut})_2$ showing 50% thermal ellipsoids. Hydrogen atoms are omitted for clarity.

to related compounds.[12] Thus, the pyridine complex has resonances at δ 142, 36, and 8.5 ppm (Figure 1a) that can be assigned to the pyridine α-, β-, and γ-hydrogens, respectively. Similarly, the MeIm complex (Figure 1b) features resonances at δ 58.1 (α-C*H*), 35.9 (β-C*H*), 29.3 (α-C*H*), and 15.1 (N−CH_3) ppm from the coordinated MeIm ligands, while the TMEDA complex (Figure 1c) exhibits peaks at δ 108 and 86 ppm arising from the diamine methyls and methylenes, respectively. For each of the aforementioned complexes, there are only five resonances in the diamagnetic region; they have the appropriate relative intensities to be assigned to the five unique protons of the bulky benzoate ligands. The observation that there are only five benzoate resonances in the pyridine and MeIm complexes is consistent with their crystal structures showing that the benzoates are structurally equivalent. For the TMEDA complex, however, the observation of only five benzoate resonances indicates that the monodentate and bidentate benzoates in this complex must interconvert rapidly on the NMR time scale. The NMR spectrum of the 2-picoline complex can be assigned by analogy to the other complexes above, but those of the two lutidine complexes are more difficult to interpret. The bulky benzoate ligand in the latter complexes gives rise to more signals than the five observed in the previous complexes, suggesting that the symmetry of the benzoate has been disrupted. While specific assignments of the NMR signals for these complexes will require further experiments (e.g., atom substitution), the adoption of structures different from those characterized in the solid state and/or a fluxional process(es) is indicated.

Discussion

We have found for the $(Mes_2ArCO_2)_2Fe(base)_2$ series that simple variation of the base results in several different structural

(12) (a) Chiou, Y.-M.; Que, L., Jr. *Inorg. Chem.* **1995**, *34*, 3270−3278. (b) Chiou, Y.-M.; Que, L., Jr. *J. Am. Chem. Soc.* **1995**, *117*, 3999−4013. (c) Borovik, A. S.; Hendrich, M. P.; Holman, T. R.; Münck, E.; Papaefthymiou, V.; Que, L., Jr. *J. Am. Chem. Soc.* **1990**, *112*, 6031−6038. (d) Zang, Y.; Kim, J.; Dong, Y.; Wilkinson, E. C.; Appelman, E. H.; Que, L., Jr. *J. Am. Chem. Soc.* **1997**, *119*, 4197−4205.

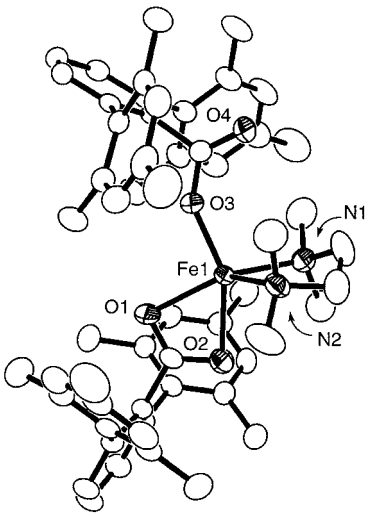

Figure 5. Drawing of the X-ray structure of $(Mes_2ArCO_2)_2Fe(TMEDA)$ showing 50% thermal ellipsoids. Hydrogen atoms are omitted for clarity.

types in the solid crystalline state. Shown in Table 1 are four representatives of those types drawn above the corresponding bases used to prepare them. Notwithstanding the ubiquitous influence of crystal packing forces on molecular structures, trends among the structures that may be rationalized by more specific metal−ligand interactions are apparent. The most obvious trend is observed for the monodentate bases, where the degree of steric bulk in the α-position correlates with the observed complex geometry. For the least hindered N-donors, MeIm and Py, the Fe center is close to tetrahedral with the carboxylates adopting monodentate binding modes. This low coordinate geometry for carboxylate-rich Fe(II) complexes is rare; to our knowledge the only closely related complex is the 5-coordinate (XDK)Fe(Py)$_2$,[8e,13] which features one monodentate carboxylate with the other bound in an asymmetric fashion with a long Fe−O interaction of 2.326(5) Å.

Increasing the steric bulk of the base by the addition of a single α-Me group results in a counterintuitive structural change. While increasing steric bulk around a metal center typically results in the lowering of the coordination number, just the opposite was observed. A comparison of bond lengths for $(Mes_2ArCO_2)_2Fe(2\text{-Pic})_2$ and $(Mes_2ArCO_2)_2Fe(2,5\text{-Lut})_2$ with the aforementioned tetrahedral derivatives makes the effect of the α-Me group apparent. It creates a steric interaction with the Fe, forcing the Fe−N bond to lengthen by about 0.1 Å.[12d,14] We hypothesize that this weakened interaction increases the Lewis acidity of the Fe, such that binding of additional ligand donors (here, bidentate coordination of the carboxylates) becomes favored. The addition of a second α-Me group (i.e., 2,6-Lut) further weakens the Fe−N interaction. However, the 2,6-Lut groups adopt trans positions, possibly to minimize steric interactions between the hindered 2,6-Lut ligands, and the carboxylates become symmetrically chelated.

A key point to be taken from the solid state structural analysis of the monodentate base series is that the carboxylate binding mode and overall stereochemistry appear to be controlled by varying the Lewis acidity of the Fe center. This variation in Lewis acidity was accomplished indirectly by changing the degree of α-substitution in a set of monodentate bases. We acknowledge that fluxional behavior and/or adoption of alternative structures in solution in some cases, as well as the operation of unspecified crystal packing forces in the solids, are important caveats. Related studies of diiron complexes have revealed similar effects wherein carboxylate binding mode differences are observed in complexes with divergent steric repulsions or N-donors.[8e,f] These findings are especially relevant to our results and suggest a generality to the notion of controlling carboxylate binding through subtle modification of Lewis acidity at the metal center.

In addition to the monodentate bases, we have also studied a derivative of the bidentate TMEDA. The use of this base introduces changes in steric bulk, donor ability, and geometry that complicate straightforward comparisons to the previous results. The ethylenediamine backbone results in a relatively fixed N−Fe−N angle (82.65(8)°) that is considerably smaller than the related values for the other complexes (Table 1). This "tying back" of the N-donors is expected to favor higher coordination number species. Moreover, the Fe−N bond lengths of $(Mes_2ArCO_2)_2Fe(TMEDA)$ (average 2.191 Å) are comparable to those of the 2-Pic and 2,5-Lut derivatives. From these data, we may simplistically expect bidentate carboxylates to be favored. What is observed, however, is a 5-coordinate species with one monodentate and one bidentate carboxylate. Most likely, the considerable steric bulk of the tetra(methyl)-substituted base prevents the bidentate coordination of both carboxylates.

In summary, the sterically hindered benzoate ligand $Mes_2ArCO_2^-$ has allowed us to access a range of new mononuclear Fe(II) carboxylates. Structural analysis of the monodentate base series has revealed the effect of N-donors on carboxylate binding mode. The simple 0.1 Å change in Fe−N distance from ca. 2.1 to 2.2 Å upon α-methyl substitution of the N-donors correlates with a shift of the carboxylates from a monodentate to a bidentate binding mode. We surmise that this change is due to an electrostatic effect, and is driven by increasing the Lewis acidity of the Fe center. Such a simple process for inducing carboxylate shifts[4] could play a critical role in biological systems that require control of coordination sites. Thus, our results in conjunction with those of others[8] suggest that a subtle conformational change in a protein could result in the necessary lengthening or shortening of a metal−nitrogen bond, thereby altering the preferred carboxylate binding mode during catalysis.

Acknowledgment. We gratefully acknowledge the National Institutes of Health for funding (GM38767 to L.Q.) and a postdoctoral fellowship (F32-GM19374 to J.R.H.).

Supporting Information Available: X-ray crystallographic files in CIF format for all new complexes. This material is available free of charge via the Internet at http://pubs.acs.org.

IC000531O

(13) XDK is the dicarboxylate ligand based on *m*-xylylenediamine-bis-(Kemp's triacid)imide.

(14) Constable, E. C.; Baum, G.; Bill, E.; Dyson, R.; van Eldik, R.; Fenske, D.; Kaderli, S.; Morris, D.; Neubrand, A.; Neuburger, M.; Smith, D. R.; Wieghardt, K. *Chem. Eur. J.* **1999**, *5*, 498−508.